Available online at www.sciencedirect.com

SciVerse ScienceDirect

Procedia - Social and Behavioral Sciences 80 (2013) 940 – 959

Procedia
Social and Behavioral Sciences

20th International Symposium on Transportation and Traffic Theory (ISTTT 2013)

Examining factors of walking disutility for microscopic pedestrian model – A virtual reality approach

Takamasa Iryo[a]*, Miho Asano[b], Shinta Odani[c] and Shogo Izumi[a]

[a]*Kobe University, 1-1 Rokkodai-cho, Nada-ku, Kobe, 657-8501, Japan*
[b]*Nagoya University, Furo-cho, Chikusa-ku, Nagoya, 464-8603, Japan*
[c]*Kyoro Prefecture, 2586-2 Yoshihara, Miyatsu-shi, Kyoto, 626-0044, Japan*

Abstract

Understanding mechanisms of microscopic pedestrian behaviour is important for pedestrian simulation, which is a useful tool for the design of pedestrian infrastructure. Interest in understanding pedestrian walking behaviour is also increasing in the mechanical engineering area to develop personal mobility vehicles that can move together with pedestrians. Like other behaviour in transport contexts, pedestrian behaviour can be modelled by the disutility minimisation principle. The property of a disutility-based model depends on how its disutility is formulated. A point of this issue is that whether pedestrians anticipate the disutility that they will experience in the next few seconds or just think of the instantaneous disutility at each moment to decide how they walk. The purpose of this study is to investigate whether the anticipation of disutility is an essential factor in a microscopic pedestrian model. Two approaches were employed for this purpose: a theoretical approach with optimal control theory and numerical calculations, and an experimental approach with a virtual reality (VR) system, in which an actual human walks through a crowd simulated by a pedestrian model. We found two main results. First, a conventional form of the social force model can be derived by instantaneous-disutility-minimisation principle. Second, actual pedestrians seem to anticipate disutility to be experienced in near future (e.g. a few seconds) to decide how to walk.

Keywords: microscopic pedestrian model; anticipation; untility maximisation principle; vitrual reality

1. Introduction

Pedestrian simulation is a useful tool for the design of pedestrian infrastructure. Its aim is to evaluate the movement of pedestrians in many places, such as public facilities, where heavy crowds are expected. Estimating the level of service of such facilities through a simulation beforehand is helpful in the construction of an effective

* Corresponding author. Tel.: +81-78-803-6360; fax: +81-78-803-6360.
E-mail address: iryo@kobe-u.ac.jp

doi:10.1016/j.sbspro.2013.05.051

geometric plan for them. Designing a good plan for pedestrian facilities is important to not only improve the level of service under normal conditions but also to prevent crowd accidents in such facilities by estimating their capacities before they are in service. Interest in understanding pedestrian walking behaviour is also increasing in the field of mechanical engineering to develop personal mobility vehicles that can move in a two-dimensional space together with pedestrians. As personal mobility vehicles are expected to be used as a mode that enhances pedestrians' activity area, smooth movement in a crowd through the avoidance of pedestrians is desired so that these vehicles can be used in the real world.

Pedestrian models describe pedestrian flow or movements, and they can be classified as macroscopic or microscopic. Macroscopic models describe crowds by using fluid dynamics as an analogy [1, 2, 3]; this approach is commonly employed in traffic flow models of vehicles on roads. In a macroscopic model, relationships between macroscopic state variables such as density, speed, and flow volume must be externally defined to describe the behaviour of a flow. Models describing these relationships (e.g. fundamental diagrams) have already been established and are widely used for vehicular traffic that moves in one-dimensional space (i.e. single roads).

For a pedestrian flow or any flow moving in a two-dimensional space, constructing general relationships among the variables describing the state of the flow is not a trivial task because the interaction between flows moving towards different directions is not simple. Although there have been a couple of studies that have analysed the interactions of bi-directional flows (i.e. interactions of flows traversing in opposite directions) [4], the general relationship of flows traversing in various directions has not been clarified. In addition, the complexity of the geometric structure of a two-dimensional space can also cause difficulties in the construction of a macroscopic model. The walking areas of these facilities have a wide variety of geometric structures owing to obstacles such as pillars. Helbing et al. [5] found that even a single pillar in front of the exit significantly improves the capacity of the exit. Macroscopic models cannot fully represent the effect of such obstacles *a priori*.

Microscopic models have the potential to resolve the disadvantages of macroscopic models by modelling how each individual pedestrian walks in a crowd without colliding against other pedestrians. The microscopic models often employ hierarchical structure to describe whole movements of pedestrians from their origins to destinations. Hoogendoorn and Bovy [6] proposed three behavioural levels consisting of 'strategic', 'tactical' and 'operational' levels. Among them, the walking behaviour to avoid collisions against other pedestrians is modelled in the operational level, whereas route-choice behaviour to select optimal routes is modelled in the tactical model, which is a higher model than the operational model. In the present study, only the operational level is focused on, in which pedestrians movements are formulated so that they can walk towards their desired directions that are externally given without colliding with other pedestrians. The desired directions are to be given by a tactical model such as Hoogendoorn and Bovy [6] – the details of tactical models are out of the scope of this study.

A few studies on microscopic pedestrian models assumed the 'utility maximisation principle' or 'disutility minimisation principle'. This approach seems to be adequate because pedestrians are human beings who may make decisions to maximise their satisfaction or minimise their discomfort while travelling. It is also consistent with many existing travel behaviour models in transport studies, especially traffic assignment models that often employed Wardop's first principle [7]. Pedestrian models can be also regarded as traffic assignment models, and hence consistency with the traditional road traffic assignment models would be preferable to preserve theoretical structure that is compatible to the traditional transport models. The utility maximisation/disutility minimisation approach also has the potential to include various (dis)utility components to explain complicated decision-making processes in many situations *a priori*, including hypothetical situations that have not been realised in the real world (e.g. evaluation of a hi-tech tool to control pedestrian flow before installation, or examination of the performance of a new personal mobility vehicle that can move around in two-dimensional space). Note that, in the following, we use the terms of 'maximising utility' and 'minimising disutility' interchangeably because they are identical.

Several assumptions can be considered to formalise the disutility of pedestrians. In an existing study [8], the components of 'drifting disutility', 'proximity disutility', and 'acceleration disutility' have been considered as

basic factors that affect the behaviour of the pedestrians. Drifting disutility is the cost caused by the difference between the desired velocity (i.e. velocity towards a pedestrian's destination) and current velocity of the pedestrian. This disutility is based on a pedestrian's behaviour in reaching his/her destination as early as possible. Proximity disutility describes discomfort when pedestrians get closer to other pedestrians or obstacles. This disutility explains avoidance behaviour. Acceleration disutility is the cost of changing the velocity.

Proximity disutility changes over time because pedestrians move. Consequently, a pedestrian should anticipate the motion of his/herself and other pedestrians in future (e.g. a few seconds) to minimise the *anticipated* disutility of walking. Thus, pedestrian movement models employing the disutility minimisation principle are expected to explicitly consider the anticipatory behaviour of pedestrians if pedestrians are assumed to consider the anticipated disutility of walking to decide their movement while walking. On the other hand, if pedestrians are assumed to consider the *current* status only and neglect all situations that will be realised in the next few seconds, pedestrians' movements should be modelled by incorporating only the *instantaneous disutility* of walking (i.e. disutility that only depends on situations such as positions of pedestrians at each time moment. Note that it does not explicitly depend on any factors that will be realised in future). Such an instantaneous decision-making process seems to be too short-sighted compared to models that consider the disutility that pedestrians will experience in future. Nevertheless, the arguments over these two assumptions—i.e. whether people consider the *anticipated disutility* or *instantaneous disutility*—should be resolved to improve the quality of the microscopic pedestrian models (note that a duration of a few seconds is not instantaneous for pedestrians because they can move a few metres within this time!). In the rest of this paper, we refer to the model considering *anticipated disutility* of walking as an 'anticipated disutility model' and refer to the model considering *instantaneous disutility* as an 'instantaneous disutility model'.

The social force model (SF model) [5, 9, 10, 11, 12, 13, 14, 15], which is a well-known microscopic simulation model, can be classified as an instantaneous disutility model if it satisfies certain condition (called 'conventional' in this paper, whose definition is denoted later). The basic concept of this model is that pedestrians experience an attractive force towards the destination and a repulsive force from surrounding pedestrians. The relationship between the SF model and the disutility minimisation principle was investigated by Hoogendoorn and Bovy [8]; their results indicated that the SF model can be mathematically derived from the disutility minimisation principle. However, as we show later in Section 2.1, the conventional SF model can be actually derived by assuming that pedestrians consider the *instantaneous disutility* only and neglect any disutility in future. The definition of the word 'conventional' for the SF model in this study is as follows. When a SF model is conventional, this model assumes a repulsive force that does not depends on any variables excluding positions of pedestrians (including surrounding pedestrians). For example, if the force depends on velocities of other pedestrians in a SF model, it is no longer conventional.

A few studies explicitly analysed anticipatory behaviour, such as Suma et al. [16] (using a cellular automata model), although microscopic pedestrian models that explicitly incorporate the anticipated disutility of travel are not in majority. Asano et al. [17, 18] proposed a model that describes the movement of pedestrians who anticipate other pedestrians' movements for a certain time horizon (e.g. a few seconds) and decide their behaviour so as to minimise walking disutility during the time horizon. This model assumes that a pedestrian receives lower disutility if he/she can proceed towards the desired direction, whereas he/she receives positive infinite disutility when he/she collides with another pedestrian or obstacle. Except for this collision disutility, no proximity disutility is considered in this model. Owing to this definition of the disutility, the pedestrian seeks a trajectory to approach the destination as fast as possible without colliding with other pedestrians or obstacles (i.e. pedestrians try to find a fastest route with no collision against another pedestrian). This model is referred to as the 'fastest trajectory model (FT model)'. An explicit formulation of future pedestrians' movements is also conducted in [19]

Instead of the explicit incorporation of the anticipatory behaviour into the model, the implicit consideration of the anticipations would be possible by considering a simpler model than that including an explicit anticipation mechanism. Johansson et al. [13] proposed such a model as an extension of the SF model. In this model (called

'Elliptical Specification II' in the above-cited paper), the proximity disutility is subject to the relative velocities of surrounding pedestrians—a pedestrian approaching to another pedestrian feels larger disutility than that diverting from another pedestrian. This mechanism implies that a pedestrian *anticipate* future collisions and change his/her course so as to avoid it. Although this model is based on the SF model, such an extension seems to implicitly incorporate the anticipatory behaviour, and hence we also regard such models as the anticipated disutility models. Some of newer SF models including Lakoba et al. [11] and Parisi et al. [14] also incorporated the effect of the relative velocities. We call such models as 'non-conventional' SF models.

The purpose of this study was to investigate whether the 'anticipated disutility' is an essential factor in determining the disutility of a pedestrian in a microscopic pedestrian model derived from the disutility minimisation principle. Two approaches were employed for this purpose: a theoretical approach with optimal control theory and numerical calculations, and an experimental approach with a virtual reality (VR) system, in which an actual pedestrian (referred to as the 'VR participant') joins a crowd generated by a simulation model through the VR system comprising an image processing computer, video projectors, screens, and motion sensors. Using a VR system for pedestrian behaviour studies is not very new; there are a few studies that have used the VR technique to investigate microscopic pedestrian models [20, 21]. Nevertheless, VR is still a state-of-the art approach in this area of study.

The VR experiment has a few advantages over an experiment involving the hiring of many people to walk in the designated study area. One is that the VR can easily compare the movements of an actual participant (i.e. a real human) and those generated by a microscopic pedestrian model in a well-controlled environment. For the VR experiment performed in this study, a VR participant was asked to walk through a crowd consisting of pedestrians generated by a simulation model. Then, in exactly the same situation, the VR participant was replaced with a simulated pedestrian (referred to as 'simulated participant'), and the same simulation was run using the same parameters. By comparing the movement of the VR participant with that of the simulated participant, we were able to examine how closely the pedestrian model can reproduce the behaviour of real humans in the VR experiment.

This paper consists of six sections, including the introduction. Section 2 includes theoretical preliminaries before the VR experiment. In Section 2.1, it will be shown that the conventional SF model can be classified into the instantaneous disutility model. Section 2.2 examines trajectories created by several models including both the instantaneous disutility models and the anticipated utility models to observe how the anticipatory behaviour changes pedestrians walking behaviour. Section 3 explains the details of the VR system and the design of the VR experiment, including the explanation of the pedestrian models used in the experiment. Section 4 shows travel time distribution of the VR experiments to exhibit the outline of its results. Section 5 compares the VR and simulated participants' movements. Finally, Section 6 discusses the effects of anticipating utility of walking and presents the conclusions.

2. Disutility Minimisation Principle and Social Force Model

In this section, it is investigated whether the conventional SF model can be derived from the instantaneous disutility model or not. The basic concept of the analysis is based on the study by Hoogendoorn and Bovy [8], that is, the disutility of a pedestrian (referred to as 'subject pedestrian') consisting of proximity disutility, drifting disutility and acceleration disutility is first defined. Then, using the optimal control theory, trajectory of the subject pedestrian is calculated so that his/her disutility is minimised. The main difference from the analysis of Hoogendoorn and Bovy is that the movements of surrounding pedestrian in future are explicitly considered in the term of the proximity disutility (i.e. the proximity disutility function explicitly depends on positions of all pedestrians in future time). By employing this formulation, the anticipatory behaviour can be incorporated in the utility function. Note that, throughout this study, it is assumed that pedestrians are selfish who only try to minimise their own disutility without thinking of others' disutility at all.

2.1. Derivation of the conventional social force model from the disutility minimisation principle

Consider a subject pedestrian who wish to walk at the velocity $\mathbf{v}^*$, referred to as 'desired velocity'. His/her initial velocity at time 0 (current time) is denoted by $\mathbf{v}_0$. The subject pedestrian will select his/her acceleration rate $\mathbf{a}(t)$ from time 0 to time when he/she finishes walking so that the disutility for walking is minimised. In the following, we only consider the case in which the desired velocity is constant while walking. Let the disutility function of a subject pedestrian consist of 'proximity disutility', 'drifting disutility', and 'acceleration disutility' over the duration of trip from time 0 to ∞, which is defined as:

$$I(\mathbf{x},\mathbf{v},\mathbf{a}) = \int_0^\infty e^{-rt}(\Phi(\mathbf{x}(t);t) + 0.5(\mathbf{v}(t)-\mathbf{v}^*)^2 + 2\tau^2 \,|\,\mathbf{a}(t)\,|^2)\mathrm{d}t\,, \tag{1}$$

where $\mathbf{x}(t)$, $\mathbf{v}(t)$, $\mathbf{a}(t)$ are the position, velocity, and acceleration vector of the subject pedestrian at time t respectively, $\Phi(\mathbf{x};t)$ is the proximity disutility caused by surrounding pedestrians and obstacles at time t, and τ, r are positive constants. Note that the proximity disutility only depends on the distances between other pedestrians and the position of the subject pedestrian. r is the temporal discount rate of the disutility. If r is greater, the subject pedestrian mostly consider the instantaneous disutility at time t. If r is smaller, he/she also considers the disutility to be experienced in the future (i.e. he/she considers anticipated disutility). τ represents the strength of acceleration disutility shown in the third term of the integral in Eqn. (1). The coefficient of the drifting disutility, which appears in the second term of the integral in Eqn. (1), is set to 0.5 without the loss of generality.

The optimal control problem to determine the trajectory that the subject pedestrian plans is defined as follows:

$$\underset{\mathbf{a}}{\mathrm{Min.}}\, I \quad \text{subject to: } \mathbf{v}(t) = \dot{\mathbf{x}}(t),\ \mathbf{a}(t) = \dot{\mathbf{v}}(t) \quad \forall t \geq 0\,, \tag{2}$$

where the dot represents the differentiation by t. The Hamiltonian corresponding to Eqn. (2) is:

$$H(t) = e^{-rt}(\boldsymbol{\lambda}(t)\cdot\mathbf{v}(t) + \boldsymbol{\mu}(t)\cdot\mathbf{a}(t) + \Phi(\mathbf{x}(t);t) + 0.5(\mathbf{v}(t)-\mathbf{v}^*)^2 + 2\tau^2\,|\,\mathbf{a}(t)\,|^2)\,, \tag{3}$$

where $e^{-rt}\boldsymbol{\lambda}(t)$ and $e^{-rt}\boldsymbol{\mu}(t)$ are the Lagrangian multipliers corresponding to $\mathbf{v}(t)$, $\mathbf{a}(t)$, respectively. Note that the discount function e^{-rt} is already applied to these multipliers to simplify the following analysis.

From Pontryagin Minimum Principle, the necessary condition for the optimal solution of Eqn. (2) can be stated as the following four equations:

$$\partial_{\mathbf{x}} H = e^{-rt}\partial_{\mathbf{x}}\Phi(\mathbf{x}(t);t) = -(e^{-rt}\boldsymbol{\lambda}(t))' = e^{-rt}(r\boldsymbol{\lambda}(t) - \dot{\boldsymbol{\lambda}}(t)) \tag{4}$$

$$\partial_{\mathbf{v}} H = e^{-rt}(\boldsymbol{\lambda}(t) + (\mathbf{v}(t)-\mathbf{v}^*)) = -(e^{-rt}\boldsymbol{\mu}(t))' = e^{-rt}(r\boldsymbol{\mu}(t) - \dot{\boldsymbol{\mu}}(t)) \tag{5}$$

$$\partial_{\mathbf{a}} H = e^{-rt}(\boldsymbol{\mu}(t) + \tau^2\mathbf{a}(t)) = 0 \tag{6}$$

$$\boldsymbol{\lambda}(\infty) = 0, \boldsymbol{\mu}(\infty) = 0, H(\infty) = 0\,. \tag{7}$$

Note that Eqn. (7) is stated to satisfy the terminal condition in Pontryagin Minimum Principle (note that no terminal cost is assumed). From Eqns. (4), (5), and (6), the following equations are derived:

$$\partial_{\mathbf{x}}\Phi(\mathbf{x}(t);t) = r\boldsymbol{\lambda}(t) - \dot{\boldsymbol{\lambda}}(t) \tag{8}$$

$$\boldsymbol{\lambda}(t) + (\mathbf{v}(t)-\mathbf{v}^*) = r\boldsymbol{\mu}(t) - \dot{\boldsymbol{\mu}}(t) \tag{9}$$

$$\boldsymbol{\mu}(t) + 4\tau^2\mathbf{a}(t) = \mathbf{0} \tag{10}$$

$\partial_{\mathbf{x}}\Phi(\mathbf{x}(t);t)$ in Eqn. (8) is replaced by $-\mathbf{f}(t)$ to convert it to an inhomogeneous ordinary differential equation (ODE) $\mathbf{f}(t)+r\boldsymbol{\lambda}(t)-\dot{\boldsymbol{\lambda}}(t)=0$. Its solution is (we only consider the solution satisfying condition in Eqn. (7))

$$\boldsymbol{\lambda}(t)=-\int_t^{\infty}\mathbf{f}(s)e^{r(t-s)}\mathrm{d}s \ . \tag{11}$$

Substituting (11) into Eqn. (9) and applying (10),

$$4r\tau^2\mathbf{a}(t)=\left\{\int_t^{\infty}\mathbf{f}(s)e^{r(t-s)}\mathrm{d}s+(\mathbf{v}^*-\mathbf{v}(t))\right\}+4\tau^2\dot{\mathbf{a}}(t) \tag{12}$$

is obtained as the ODE for solving $\mathbf{v}(t)$ and $\mathbf{a}(t)$. The homogeneous ODE corresponding to (12) is

$$\mathbf{v}(t)+4r\tau^2\mathbf{a}(t)-4\tau^2\dot{\mathbf{a}}(t)=0\,. \tag{13}$$

Note that $\mathbf{a}(t)=\dot{\mathbf{v}}(t)$ is already applied. The solution of ODE (13) is

$$\mathbf{v}_+(t)=e^{p_+t},\mathbf{v}_-(t)=e^{p_-t} \quad \text{where } p_+=0.5r\left(1+\gamma\right),\ p_-=0.5r\left(1-\gamma\right),\gamma=\sqrt{1+\alpha},\alpha=(r\tau)^{-2} \tag{14}$$

excluding the arbitrary constant. Hence, the general solutions of the original inhomogeneous ODE in (12) is

$$\mathbf{v}(t)-\mathbf{v}^*=\tau^{-2}\gamma^{-1}\left\{e^{p_-t}\int\mathbf{g}(t)e^{-p_-t}\mathrm{d}t-e^{p_+t}\int\mathbf{g}(t)e^{-p_+t}\mathrm{d}t\right\} \quad \text{where } \mathbf{g}(t)=\int_t^{\infty}\mathbf{f}(s)e^{r(t-s)}\mathrm{d}s \tag{15}$$

Among the general solutions of (15), the solution consisting no divergent term is:

$$\mathbf{v}(t)-\mathbf{v}^*=0.25\tau^{-2}\gamma^{-1}\left\{\mathbf{G}_-(t)+\mathbf{G}_+(t)\right\}+\mathbf{c}_0e^{p_-t}, \tag{16}$$

where

$$\mathbf{G}_-(t)=\int_0^t\mathbf{g}(s)e^{p_-(t-s)}\mathrm{d}s,\ \mathbf{G}_+(t)=\int_t^{\infty}\mathbf{g}(s)e^{p_+(t-s)}\mathrm{d}s \tag{17}$$

and the constant vector $\mathbf{c}_0$ is set so that $\mathbf{v}(0)=\mathbf{v}_0$ is satisfied. By differentiating both side of (16), we obtain

$$\mathbf{a}(t)=0.25\tau^{-2}\gamma^{-1}\left\{p_-\mathbf{G}_-(t)+p_+\mathbf{G}_+(t)\right\}+p_-\mathbf{c}_0e^{p_-t}\,. \tag{18}$$

Combining Eqns. (16) and (18),

$$\mathbf{a}(t)=0.25\tau^{-2}\mathbf{G}_+(t)-p_-(\mathbf{v}^*-\mathbf{v}(t)) \tag{19}$$

is obtained, which corresponds to the equation of the SF model if $\mathbf{G}_+(t)$ is interpreted as the force that the subject pedestrian experiences. Note that, as $p_- < 0$, the coefficient of the second term is positive, implying that the second term represents the force that let the subject pedestrian move toward his/her desired velocity.

We finally show that the conventional SF model is identical to the instantaneous utility model. First, $\mathbf{G}_+(t)$ defined by (17) can be re-written as follows:

$$\mathbf{G}_+(t) = \int_t^\infty \left\{ \int_s^\infty \mathbf{f}(u) e^{r(s-u)} \mathrm{d}u \right\} e^{0.5r\left(1+\sqrt{1+(r\tau)^{-2}}\right)(t-s)} \mathrm{d}s \,. \tag{20}$$

When pedestrians only consider the instantaneous disutility so that $r\tau$ is sufficiently greater than 1 and $e^{r(t-u)}$ converges to 0 quickly before $\mathbf{f}(u)$ changes, (20) can be approximated to:

$$\mathbf{G}_+(t) = \int_t^\infty \left\{ \int_s^\infty \mathbf{f}(u) e^{r(s-u)} \mathrm{d}u \right\} e^{r(t-s)} \mathrm{d}s = \int_t^\infty \int_s^\infty \mathbf{f}(u) e^{r(t-u)} \mathrm{d}u \mathrm{d}s = \mathbf{f}(t) \int_t^\infty \int_s^\infty e^{r(t-u)} \mathrm{d}u \mathrm{d}s = r^{-2} \mathbf{f}(t) \,. \tag{21}$$

And applying $p_- = 0.5r(1-\sqrt{1+(r\tau)^{-2}}) \simeq -0.25r(r\tau)^{-2}$, we obtain the approximated form of

$$\mathbf{a}(t) = 4(r\tau)^{-2} \left\{ \mathbf{f}(t) + r(\mathbf{v}^* - \mathbf{v}(t)) \right\} \tag{22}$$

for the equation of motion, which is exactly compatible to the conventional social force model. Meanwhile, when pedestrians also incorporate the change of $\mathbf{f}(u)$ for a few seconds after time t to anticipate walking disutility (i.e. the anticipated utility model is assumed), the approximation in Eqn. (21) is no longer valid. In such a case, from Eqn, (20), it is apparent that $\mathbf{G}_+(t)$ depends on $\mathbf{f}(u)$ not only at time $u=t$ and but also time $u>t$, implying that the force depends on future movements of surrounding pedestrians. Thus, it can be concluded that the conventional social force model is identical to the instantaneous utility maximisation model and not compatible to the anticipated utility model.

2.2. Numerical test for comparison of SF models and FT model

The trajectories calculated by five SF-based models and the FT model are shown and compared in this section to understand how the anticipatory behaviour can affect pedestrians' behaviour. Table 1 shows the specifications and classifications (i.e. whether each of them is a conventional SF model or not) of these models. Note that the values of parameters not shown in this table are equal to those in the original articles.

To examine how pedestrians simulated by each model avoid collisions, a simple scenario in which two pedestrians walking to a same collision point in different directions was considered in the numerical test. In this study, the angle of the directions was set to 90 degrees. For such a setting, a qualitative analysis by Asano et al. [17] has implied that, in the conventional SF model, the two pedestrians may fail to avoid each other smoothly. Fig. 1a depicts the scenario setting. Two pedestrians were generated from point A and line B (the position of the generation is randomly determined on line B) at the same time, in which the desired direction of a pedestrian from A was the right and that from B is the upside. The desired speeds of the pedestrians were randomly set between 1.2 and 1.4 (m/s). The radius of pedestrians was 0.3 m. Two pedestrians were to collide at point C in Fig 1a unless they avoid each other. In the numerical test, 50 trials were conducted for each model.

Fig. 1b shows the trajectories generated by six models. The relative positions of the pedestrian from B to the pedestrian from A, denoted by $(\Delta x, \Delta y)$, are depicted by each graph, where $\Delta x = x_B - x_A$, $\Delta y = y_B - y_A$ and (x_A, y_A) and (x_B, y_B) are the position of the pedestrians from A and B, respectively. The dashed circles in Fig. 1b

indicates the area in which the trajectories of $(\Delta x, \Delta y)$ cannot enter (i.e. two pedestrians collide when a trajectory touches onto the dotted circle).

The result shown in Fig. 1b implies that pedestrians simulated by H1a, H1b, H2a, or H2b cannot avoid other pedestrians smoothly. Most pedestrians by the former four models approach the opponent very closely and make steep turns to avoid it. Moreover, it seems that many pedestrians seem to bounce off the opponent before starting avoiding it. These trajectories may not be typical in the real world, in which pedestrians may start the avoiding behaviour well before the collisions. On the other hand, pedestrians simulated by JH and FT start avoiding the opponent well ahead of the collision point and make smooth avoiding movements.

Owing to the analysis in Section 2.1 and the above numerical test, it can be said that behaviour of actual pedestrians may not be able to be explained by the instantaneous disutility model, implying that the instantaneous disutility is not a sole part of walking disutility and considering the anticipated disutility (either explicitly or implicitly) is necessary.

Table 1. Model Specifications

Model	Specification	Classification of SF models
H1a	Helbing et al. (2000) [10]	Conventional SF (unless collision occurs)
H1b	Helbing et al. (2000) [10], $A_i = 1.5$ (m/s^2), $B_i = 1.5$ (m)	Conventional SF (unless collision occurs)
H2a	Helbing et al. (2005) [5], $A_\alpha^1 = 0$, $\tau_\alpha = 1.0$ (s)	Conventional SF
H2b	Helbing et al. (2005) [5], $A_\alpha^1 = 0$, $\tau_\alpha = 1.0$ (s), Eyesight of each pedestrian is restricted between ϕ-60 to ϕ+60 (deg), where ϕ is desired direction.	Conventional SF
JH	Johansson et al. (2007) [13], Elliptical specification II, $A = 1.0$ (m/s^2), $B_i = 1.0$ (m), $\lambda = 1$, $\Delta t = 2.5$ (s), $\tau_\alpha = 2.0$ (s)	Non-conventional SF
FT	Fastest Trajectory Model (Asano et al., 2009) [17] , $n_{BP} = 1$	(Not a SF model)

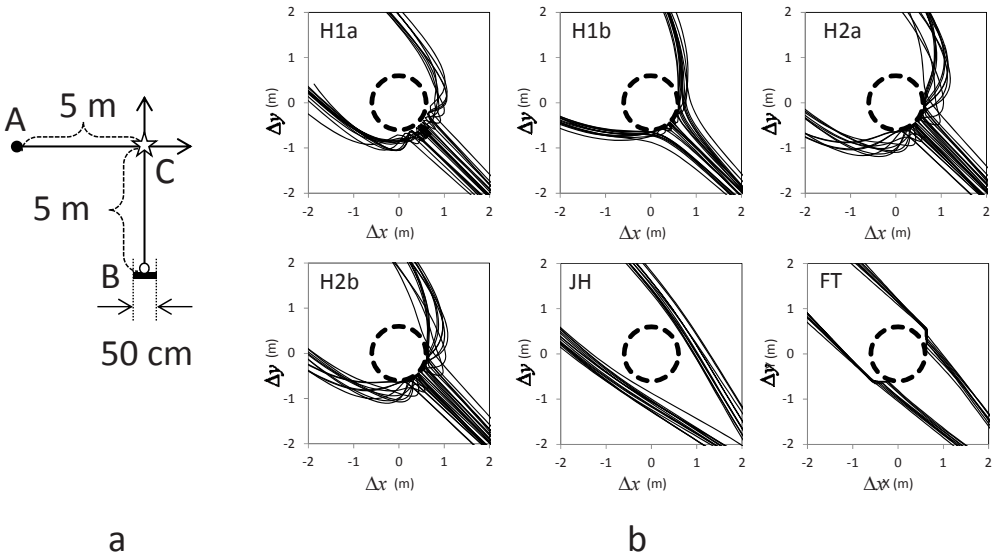

Fig. 1. (a) Scenario setting for the numerical test and (b) its results: the label on each graph in (b) indicates the model corresponding to the first raw of Table 1. Dotted circles in (b) indicates the area into which trajectories cannot enter due to the size of the body (diameter = 0.6 m).

3. Implementation of Virtual Reality System for VR experiment

3.1. Overview

This section introduces the details of the VR experiment system, in which movements of all pedestrians except a participant (VR participant) are calculated by a microscopic pedestrian model (i.e. the SF model or FT model). Before describing the details of the VR system, the reason why the VR experiment is suitable for the purpose of this study is explained. There are a few approaches to observe actual pedestrian movements. Observing pedestrian movements in the real world (including experiments in an artificial environment) is a popular approach to investigate actual pedestrian movements. This approach is suitable to observe macroscopic characteristics of a pedestrian flow (e.g. a speed-density relationship on a single corridor [22]). It can be also utilised to investigate microscopic movements of the pedestrian. Hoogendoorn and Daamen estimated parameters of a microscopic model using the data taken by an experiment [23]. Robin et al. also utilised data taken by an experiment to construct a logit model explaining pedestrian's movements [24]. These studies aimed to see how pedestrians' movements at each time step (i.e. instantaneous behaviour) are determined. Meanwhile, to examine the effect of the anticipation behaviour of pedestrians, observing behaviour at each time step independently (i.e. with no consideration of the temporal correlation) is not sufficient because the current movements may be correlated with the movements of other pedestrians in the future. Instead, we need to investigate pedestrian trajectories for certain duration of time. Investigating temporal correlations of movements of many pedestrians in a crowd is not easy – movements of pedestrians are subject to complex interactions among pedestrians including many unknown factors, implying that the extracting the mechanism of the motion from the observed data is a difficult task.

In this study, we use the VR technique in order to remedy the problem of complexity in surveying pedestrians' behaviour in a crowd. As mentioned in Section 1, the main advantage of the VR experiment is that the behaviour of a VR participant, which is an actual human, can be easily replaced by a pedestrian whose movement is calculated by a simulation. More specifically, consider an experiment in which a VR participant walks through a crowd generated by a simulation model (referred to as 'simulated crowd'). As the VR experiment is performed in a computer, we can accurately collect all the data such as trajectories of all pedestrians including the VR participant. After the experiment, we can 'restart' it from an arbitrary timing by replacing the VR participant with the simulated participant, whose movement is calculated by the simulation model that is used for generating the simulated crowd. Because the initial condition of the restarted experiment is exactly the same as that of the VR experiment, we can consider that the difference in the movements between the VR participant and the simulated participant is caused by the differences between the mechanisms of VR participant's behaviour and that of the simulation model. Such a procedure can be made because all the pedestrians in the crowd are calculated by the simulation model in the VR experiment. If the crowd consists of real humans, we need to replace all of them by the simulated pedestrians, in which the difference between actual movements and simulated movements cannot be clearly investigated.

A diagram of the VR system used in this study is shown in Fig. 2. The VR participant enters the VR box comprising of screens, projectors, and motion sensors. The VR participant watches the movements of pedestrians in a simulated crowd projected onto the screens and walks towards the destination by avoiding collision with other pedestrians in the simulated crowd. Motion sensors detect the walking speed and direction of the participant and send these data to the VR and simulation engines. Pedestrians in the simulated crowd are generated and controlled by a simulation model; their motions are affected by the movement of the VR participant.

The VR system also has a function that replaces the VR participant by the simulated participant at any arbitrary timing. This function is depicted as a 'switch' in Fig. 2. Once the switch is flipped from the left to the right (i.e. from the VR participant to the simulated participant), the simulation with the VR participant halts and the VR participant is replaced by the simulated participant. Then, the simulation with the simulated participant restarts from the timing when the simulation with the VR participant halts. This procedure is referred to as

'restarting procedure'. By performing the VR experiment beforehand, we will be able to make the restarting procedure as many times as we want at any arbitrary timing using the collected data. This procedure enables us to compare the trajectory of the VR participant with that of the simulated participant. This comparison will provide the information on how the behaviour of the real human in the VR system is different from that of the simulation model. The schematic view of the restarting procedure is shown in Fig. 3. Fig. 4 shows an example of the result by the restarting procedure. In this figure, we can see differences between the movement of the VR participant and that of the simulated participant. Note that there is also a slight difference of the movements of the pedestrians in the simulated crowd because they react to the motions of VR/simulated participant.

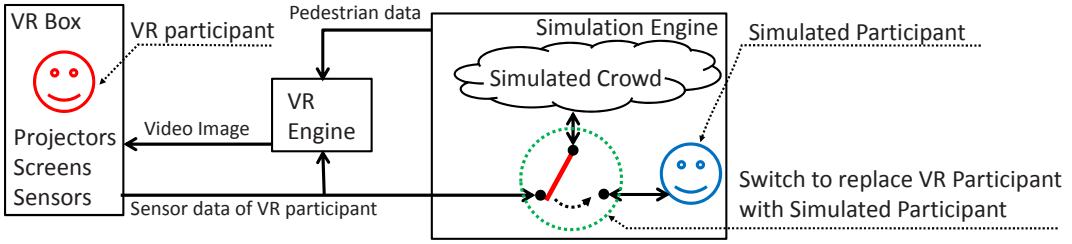

Fig. 2. Diagram of VR experiment system

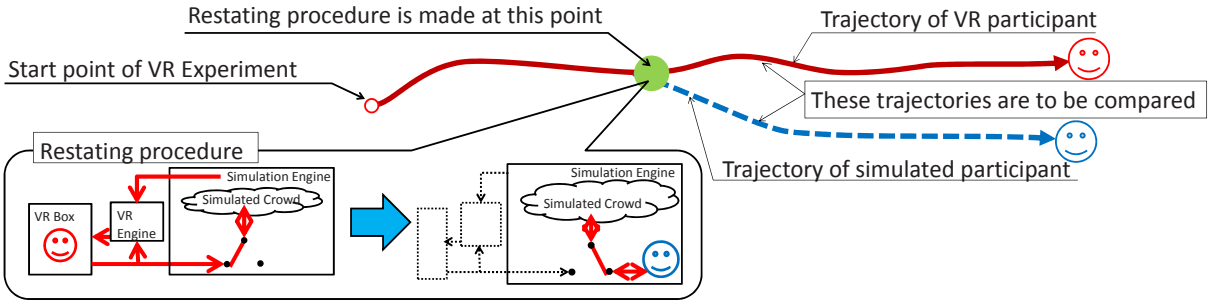

Fig. 3. Schematic view of restarting procedure

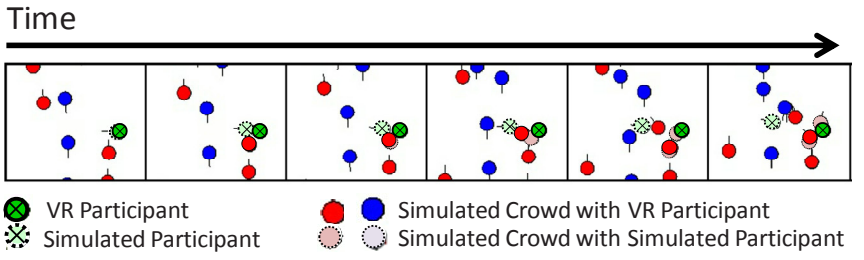

Fig. 4. Example of movements by VR participant, simulated participant, and simulated crowds after restarting procedure
(Circles in each box indicate positions of pedestrians at each time. The result of VR experiment is superposed on that of simulated participant)

3.2. Configuration of VR box

The configuration of the VR box is shown in Fig. 5(a). The VR box comprises of three screens, three projectors, and motion sensors. Three screens surrounding a VR participant provides a semi-immersive environment. Fig. 5(b) shows a picture of the VR box. Since distances between pedestrians in the real world can become less than tens of centimetres, it is important to reproduce the sense of proximity to other pedestrians. Using the transmissive projection technique, we could build a small VR box, whose width and depth are 1050 x 1050 mm. The height of the VR box is 1830 mm. Fig. 6(a) is an example of the view projected onto the screens. The view is vertically divided into two parts by a black line: the upper part is a normal projection, whereas the lower part is a 'bent view', which enables the VR participants to see the places near their foot (Fig. 6(b)). The range of the sight is more than 180 degrees for horizontal angle and around 100 degrees for vertical angle.

The VR participant steps without moving in the VR box. Two iPod touches detects his/her motions. One of them is attached to the waist to detect the direction of the participant by a built-in gyro sensor. The direction of the VR participant detected by the sensor is indicated on the screen by an arrow. The other is attached to the arm to detect the swing of the arm by a built-in acceleration sensor (we considered that swinging arms while walking is natural and also asked participants to do so). The walking speed of the VR participant is fixed to 1.3m/s; participants can adjust the speed by stopping the swinging from time to time. All the motion data is sent to the computer of the VR engine via Wi-Fi connections. Using the motion data and the data from the simulation engine, the VR engine generates the view to be projected onto the screens. To implement the VR engine, a video game library software named 'Irrlicht Engine' [25] was used.

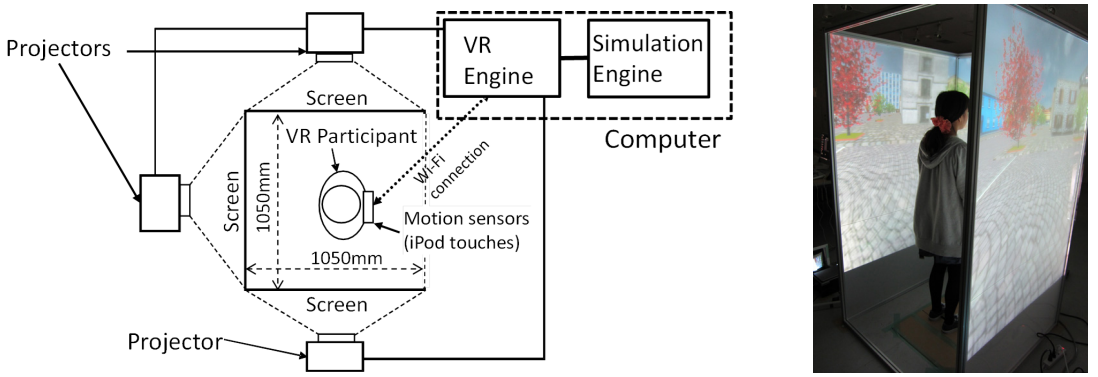

Fig. 5. (a) Configuration of VR box (left); (b) Picture of VR box (right)

Fig. 6. (a) View that is projected onto screens of VR box (left)
(b) Geometrical configuration of normal view and bent view (vertically compressed; the aspect ratio is not conserved) (right)

3.3. Pedestrian simulation models

Two simulation models were implemented to the VR system; the conventional SF model as the representative of the instantaneous disutility models and the FT model by Asano et al. [17] as the representative of the anticipated disutility models. The conventional SF model used in the experiment is identical to 'H2b' in Table 1; we simply call it as the SF model in the following sections. Pedestrian i receives the acceleration rate $\mathbf{a}_i$ calculated by the following equation:

$$\mathbf{a}_i = \alpha(\mathbf{v}_i^* - \mathbf{v}_i) + \beta \sum_{j \in N_i} \mathrm{e}^{(0.6-d_{ij})/0.2} (\mathbf{x}_i - \mathbf{x}_j)/d_{ij} \ , \tag{23}$$

where $\alpha = 1$ (/s), $\beta = 3$ (m/s^2), $\mathbf{x}_i$ is the current position, $\mathbf{v}_i$ is the current velocity, $\mathbf{v}_i^*$ is the desired velocity, d_{ij} is the distance between pedestrian i and j (note that its unit is metre) , and N_i is the set of pedestrians within the field of view of pedestrian i. The shape of the field of view is assumed to be a sector whose radius is 5 m and angle is 120 degrees. The direction of the field of view is fixed to the desired direction.

In the FT model, each pedestrian seeks a spatial-temporal trajectory (referred to as 'intended trajectory') that maximises the length of the movement along his/her desired direction for a given time horizon (5 seconds) with no collision against other pedestrians. These intended trajectories correspond to the anticipations made by the pedestrians; they represent the movement of the pedestrians in the next five seconds. In this model, each pedestrian is assumed to be able to know intended trajectories of other pedestrians within their field of view (5 m from the pedestrian). Based on this assumption, in the simulation model, the information on the intended trajectories is shared by the all pedestrians. The details of the algorithm are shown in [17]. Same parameters in the numerical test in Section 2.2 were used.

To implement the FT model on the VR system, we need to consider the fact that the VR participant cannot share the information of intended trajectories with simulated pedestrians. In the VR experiment, we assumed that the direction of the intended trajectory of the VR participant is same as the direction that the VR participant is facing. In addition, we externally set the priority (i.e. superior or inferior to the VR participant) for all pedestrians in the simulated crowd. If a simulated pedestrian is superior to the VR participant, it neglects the VR participant. Otherwise, it determines its intended trajectory that avoids the intended trajectory of the VR participants.

For both models, geometrical structure of each pedestrian was represented by a circle whose radius is 0.3 m. Simulation time step was set as 0.05 seconds. The desired speed of simulated participants was set as 1.3m/s, which is equal to that of the VR participants. The desired speeds of pedestrians in the simulated crowd were randomly set between 1.0 m/s and 1.6 m/s.

3.4. Experimental design

A simple right-angled intersection shown in Fig. 7 was employed as the walking area of the VR experiment, in which a VR participant was asked to cross the simulated crowd that moves perpendicularly to the desired direction of the VR participant. Each VR participant was asked to walk from left-hand side to right-hand (or right-hand side to left-hand side) of the experimental field. Simulated pedestrians were generated from upper and/or lower end of the corridor and go straight to the other end.

In the VR experiment, the level of proficiency to the VR system may affect the behaviour of the VR participants. To remedy this problem, the VR participants were asked to do the training programme first, which was followed by the main experiment. Two training programmes were conducted; in one programme, each participant was asked to walk in the condition surrounded by pedestrians that did not move. This programme intended to improve the control skill of walking and the sense of distance to the other pedestrians in the VR system. In the other programme, each participant was asked to cross a low-volume pedestrian flow. This was to

improve the control skill and the sense of speed. Both trainings were conducted four times.

In the main experiment, four scenarios shown in Table 2 were set. The directions of desired velocities are along to the road (i.e., upward or downward direction for the simulated crowd and leftward or rightward direction for the simulated participants) in Fig. 7. In each scenario, the VR participant was asked to cross the intersection eight times. They were asked to finish walking as fast as possible (of course, finish walking faster is identical to finish the experiment earlier, implying that they had an incentive to finish walking as fast as possible). We employed 61 participants (53 males and 8 females) for the VR experiment. All of them were students of a university – they were in the civil engineering department but no one knew the details of the pedestrian models in this study. About half of the participants (31 persons incl. 27 males and 4 females) were asked to walk in the environment of the SF model and the other half (30 persons incl. 26 males and 4 females) were walked in that of the FT model. Note that no one experienced both models – only either one model was assigned to each participant. The order of the scenario in each experiment was designed to minimise the order effect.

Each VR participant was asked to walk as usual without colliding against another pedestrian. If he/she made contact with another pedestrian continuously for 0.2 seconds, he/she was considered to have collided. Once the collision was detected, a warning message was shown on the screen for a few seconds and then he/she was forcibly moved to the start position again (i.e. he/she must start over from the start position). The participants were not informed on the details of the simulation models. Instead, they were told that the simulated pedestrians imitate the actual behaviour of pedestrians.

Trajectories of the VR participants and the pedestrians in the simulated crowd were collected for the analyses. The data when participants collided with simulated pedestrians or an edge of the roads were omitted from the data. For each scenario, 248 and 240 data sets were collected for the SF model and FT model, respectively (one data set corresponds to a trajectory data of one crossing).

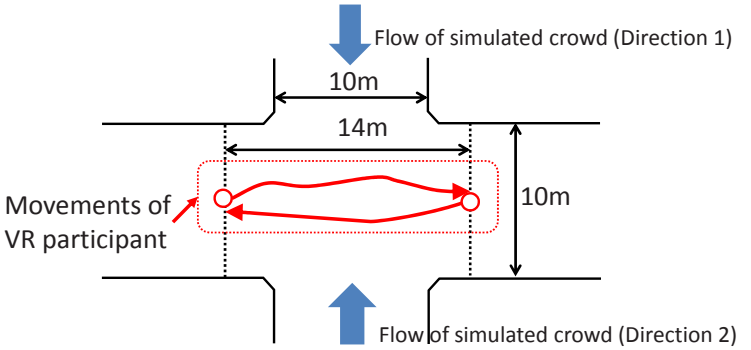

Fig. 7. Walking area in the experiment

Table 2. Scenario Settings

Scenario	Pedestrian volume (ped/minute)	Width of generated pedestrian flow
A	60 on direction 1	2 m
B	60 on both directions 1 and 2	9 m
C	100 on direction 1 and 20 on direction 2	9 m
D	120 on direction 1	9 m

4. Travel Time Distribution of the VR experiment

Travel time (i.e. time to cross the intersection) of the VR participants was employed as an index for checking participants' macroscopic behaviour. Note that, considering the speed of the VR participants (1.3m/s), minimum travel time to cross the intersection is 7.7 seconds. Fig. 8 shows the distributions of travel times of VR participants in Scenario A to D with simulated crowds by either FT or SF model. Average travel time is also shown in the figure. Compared to Scenario A, all other scenarios tend to have larger average travel time owing to larger pedestrian demand of the simulated crowd. Average travel times of the FT model are less than those of the SF model in all scenarios. By Mann–Whitney U test, it can be confirmed that the travel time of the FT models is significantly less than that of SF model at the 95% confidence level except Scenario B. This result implies that the VR participants effectively avoided pedestrians in the simulated crowd generated by the FT model as compared to those by SF model. This result is consistent with the result in Section 2.2., i.e., pedestrians simulated by the FT model can smoothly avoid other pedestrians than pedestrians simulated by the conventional SF models (i.e. models except 'JH' and 'FT'), which is identical to the instantaneous force model.

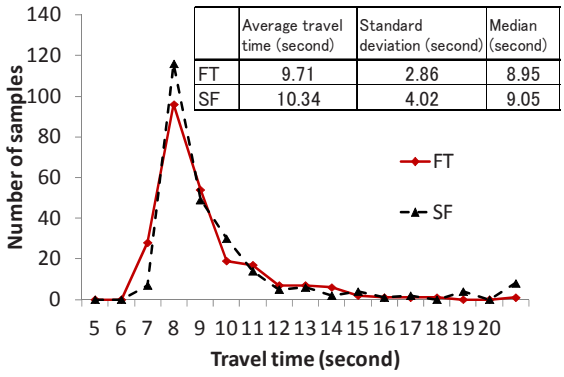

	Average travel time (second)	Standard deviation (second)	Median (second)
FT	9.71	2.86	8.95
SF	10.34	4.02	9.05

(a) Scenario A

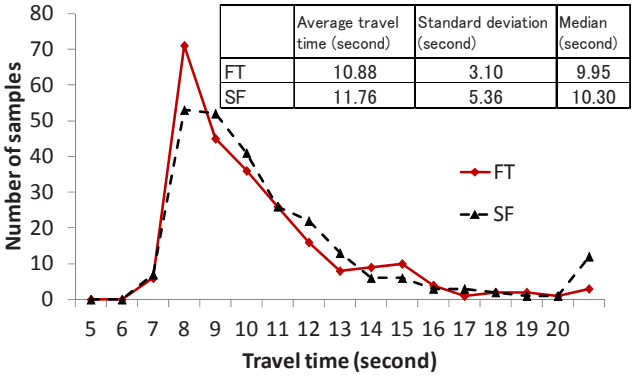

	Average travel time (second)	Standard deviation (second)	Median (second)
FT	10.88	3.10	9.95
SF	11.76	5.36	10.30

(b) Scenario B

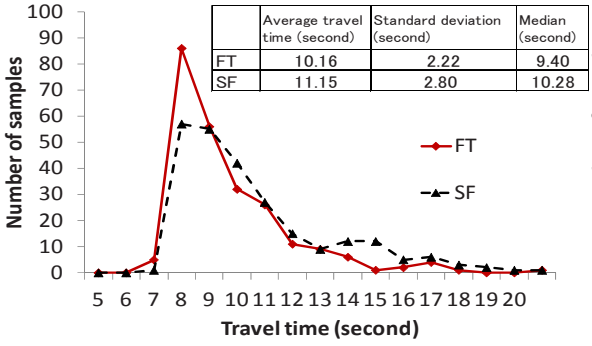

	Average travel time (second)	Standard deviation (second)	Median (second)
FT	10.16	2.22	9.40
SF	11.15	2.80	10.28

(c) Scenario C

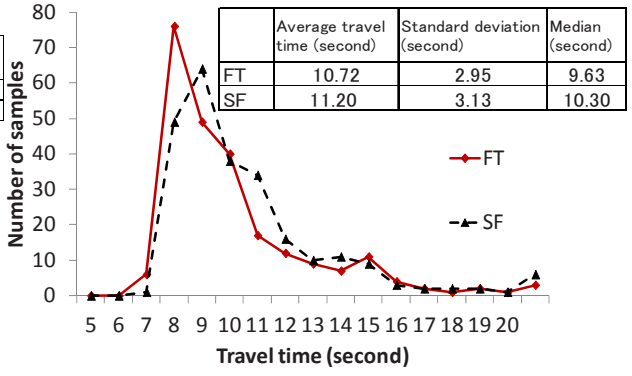

	Average travel time (second)	Standard deviation (second)	Median (second)
FT	10.72	2.95	9.63
SF	11.20	3.13	10.30

(d) Scenario D

Fig. 8. Distributions of travel time of VR participants: FT and SF indicates the model generating the simulated crowd.

5. Comparison of Movements between VR Participants and Simulated Participants

This section performs comparisons of movements between VR participants and simulated participants when they need to avoid a collision with another pedestrian in the simulated crowd. The comparison was performed by the 'restarting procedure' explained in Section 3.1.

5.1. Method of comparison

The movements of the participant (both VR and simulated) were evaluated in relationship to another pedestrian of the simulated crowd, which is referred to as 'opponent'. The opponent is defined as a pedestrian whom the participant approaches (the detailed process to select the opponent against the particular participant is explained later). Because the opponent is to be avoided by the participant, movements of the participant against the opponent represent how the participant reacts against other pedestrians' movements. Consequently, investigating the relative relationship of positions between these pedestrians should provide useful information to understand how the participant avoids collisions with other pedestrians.

To describe the relationship between the participant and the opponent, the following variables were defined:

$$\Delta x = x_p - x_o,\ \Delta y = y_p - y_o, \tag{24}$$

where (x_p, y_p) is the coordination of the participant and (x_o, y_o) is the coordination of an opponent. Further, the following modification was made to standardise the topological relationship between these pedestrians:

$$\Delta x^* = \begin{cases} \Delta x & \text{if } v^*_{ox} > 0 \\ -\Delta x & \text{otherwise} \end{cases},\ \Delta y^* = \begin{cases} \Delta y & \text{if } v^*_{py} > 0 \\ -\Delta y & \text{otherwise} \end{cases}, \tag{25}$$

where $\mathbf{v}^*_o = (v^*_{ox}, v^*_{oy})$ and $\mathbf{v}^*_p = (v^*_{px}, v^*_{py})$ are the desired velocity of the opponent and the participant, respectively. In the coordination system defined by Eqn. (25), the opponent always walks from left to right, whereas the participant always walks from bottom to upside. Fig. 9(a) is a schematic view of two pedestrians on the 2-D plane of Δx^* and Δy^*, referred to as 'Relative Coordinate (RC) Plane'. Note that, as depicted in Fig. 9(a), the desired velocity of any participant on this plane is a left-diagonal upward direction.

Any participant approaching to an opponent is always in the fourth quadrant on the RC plane. Fig. 9(b) is a schematic view to understand the relationship between a participant and an opponent. As indicated in this figure, any pedestrian on either first, second or third quadrant is not approaching the opponent staying at the origin on the plane but leave from the opponent. Only a pedestrian on the fourth quadrant will approach the opponent.

The detailed procedure to pick up an opponent and track a participant approaching to this opponent is explained in below. First, the polar coordination system is defined as

$$r = \sqrt{\Delta x^{*2} + \Delta y^{*2}},\ \theta = \tan^{-1}(\Delta y^* / \Delta x^*) \tag{26}$$

and a pair of a participant and an opponent satisfying the following relationship is picked up.

$$r = 1.2 \text{ m and } -70° \le \theta \le -20° \tag{27}$$

Note that any pedestrian in the simulated crowd can be an opponent once Eqn. (27) is satisfied. θ at $r = 1.2$ is referred to as 'Angle of Incidence' and denoted by θ_I. The time when this condition is satisfied for the first time is denoted by t_0. Then, the trajectory of this participant is tracked for the analysis till he/she exits the fourth

quadrant (i.e. ceases approaching to the opponent). The time when he/she exits the fourth quadrant is denoted by t_1. Once the participant is tracked, the tracking continues even when r becomes greater than 1.2 m. $t_1 - t_0$ is referred to as 'time for avoidance (TfA)', which describes how long the participant spends the time to finish avoiding the opponent to prevent the collision. Fig. 10 is a schematic view of the tracking procedure. The tracked trajectories of the participants on the RC plane and the relationships between the TfA and θ_I are examined for each approaching participant. To compare behaviour of VR participants and simulated participants, the following procedure was employed:

(1) Pick up a VR participant who is approaching an opponent by Eqn. (27). Denote this approach by i (note that many different pedestrians can be selected as the opponents of the same participant, implying that the approach can be made many times by one participant. Therefore, i does not correspond to each participant). Determine the enter time of approach i, denoted by $t_0(i)$, and the angle of incidence, denoted by $\theta_I(i)$.

(2) Track the trajectory of the VR participant till it exits from the fourth quadrant. Let the exit time $t_1^{VR}(i)$ and calculate TfA as $t_1^{VR}(i) - t_0(i)$.

(3) Perform the restarting procedure at time t_0 using the data of the corresponding VR experiment. Track the trajectory of the simulated participant till it exits from the fourth quadrant. Let the exit time $t_1^{SIM}(i)$ and calculate TfA as $t_1^{SIM}(i) - t_0(i)$.

This procedure was made for all experiments of all participants. Then, the difference of the TfA between each VR participant and simulated participant was calculated by:

$$\Delta T(i) = \left\{t_1^{SIM}(i) - t_0(i)\right\} - \left\{t_1^{VR}(i) - t_0(i)\right\} \quad . \tag{28}$$

$\Delta T(i)$ indicates how the TfA of the simulated participant is different from that of the VR participant. The relationships between $\Delta T(i)$ and $\theta_I(i)$ will be investigated by drawing them on the graphs.

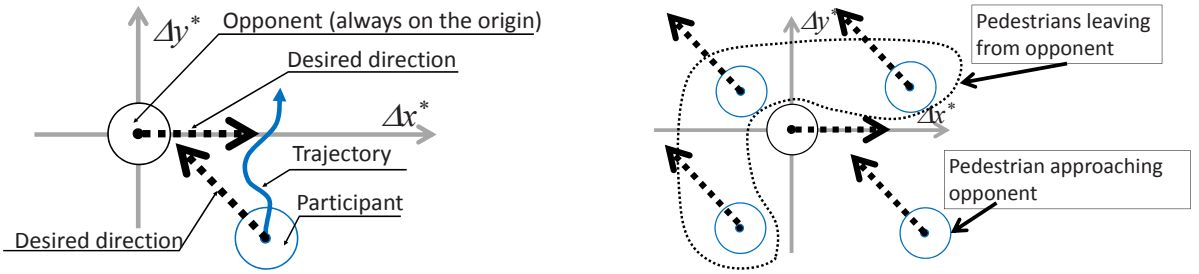

Fig. 9. (a) RC plane and participant and opponent (left); (b) Participants on each quadrant and their desired directions (right)

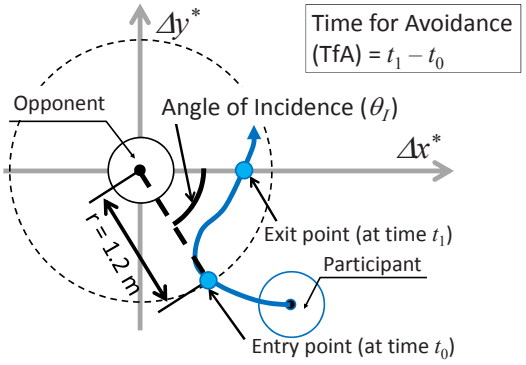

Fig. 10. Schematic view of tracking

5.2. Results of analysis

The relationships between the difference of the TfA and the angle of incidence are depicted in Figs. 11 and 12. The number of approaches is also denoted by N in the graph. N tends to be greater if the simulated crowd is dense or the SF model is used, implying that VR participants tend to approach the opponent closer than those in the crowd of the FT model. In the SF model, 1-2 seconds delay was found in TfA of the simulated participants for $-50° \le \theta_I \le -40°$. Meanwhile, there is no significant difference in the FT models. This result implies that the conventional SF model may not be able to reproduce TfA of the VR participants, while the FT model can do so.

To investigate the reason of the biases on TfA in the SF model, trajectories of the participants whose angles of incidence are between $-43°$ and $-47°$ are shown in Fig. 13 (for Scenario C only). In Fig. 13, trajectories of the simulated participants first go towards the opponent, then bounce off the opponent at around $r = 0.6$ m. The bouncing participants then leave from the opponent and draw curves like a sine curve before leaving the fourth quadrant. Fig. 14, which shows relationships between elapsed time from $t_0(i)$ and r, also supports this characteristic. It corresponds to the 'bouncing' movement exhibited in Section 2.2. It is unique to the simulated participants in the SF model. The bouncing movements are actually found for VR participants in the SF model, but they occur less frequently compared to the simulated participant case. In the FT cases, no bouncing is found for both simulated participants and VR participants. In Fig. 13, we can also observe smooth avoiding movements of the VR participants in both the SF and FT models and the simulated participants in the FT model. The relationship between elapsed time from the entry time $t_0(i)$ and θ is depicted in Fig. 15 to conform the avoiding movement. These graphs indicate that the simulated participants in the SF model always walk towards the opponent (i.e. $\theta \approx -45°$) for around 0.5 second, whereas, in all other cases, many participants rapidly change θ to $\theta \approx 0°$ or $-90°$. Comparing these results with the results of the numerical test in Section 2.2, it can be said that the instantaneous utility model is not sufficient to explain the trajectories of actual pedestrians and anticipated disutility should be incorporated into the walking disutility.

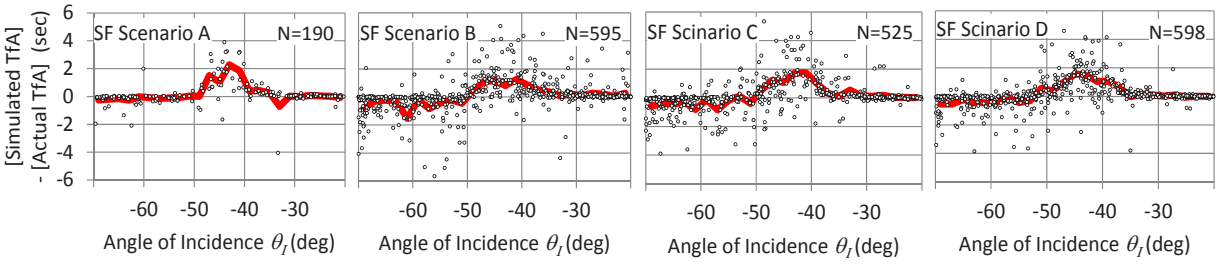

Fig. 11. Difference of TfA between VR and simulation: SF model. Dots indicate individual data. Red line indicates the average per 2 degrees. Vertical axis is common for all graphs.

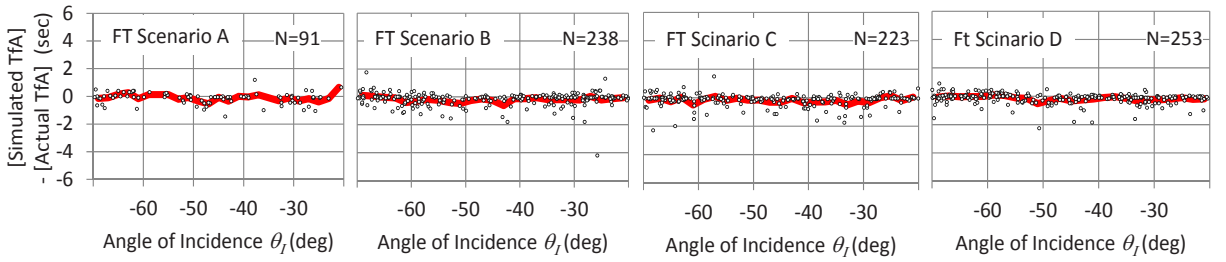

Fig. 12. Difference of TfA between VR and simulation: FT model. Dots indicate individual data. Red line indicates the average per 2 degrees. Vertical axis is common for all graphs.

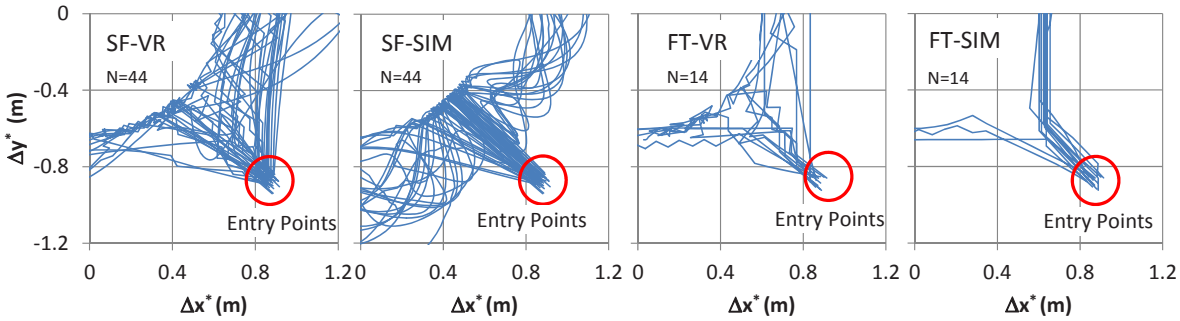

Fig. 13. Trajectories of participants in Scenario C on RC plane. Angles of incidence are between −43° and −47° (SIM = Trajectories of simulated participants, VR = Trajectories of VR participants). Vertical axis is common for all graphs.

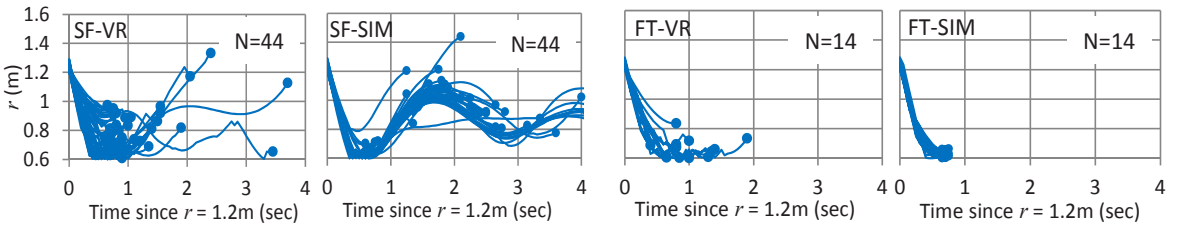

Fig. 14. Relationship between elapsed time and r. SIM = Simulated, Angles of incidence are between −43° and −47° . Scenario is C. Dots indicate exit points. Vertical axis is common for all graphs.

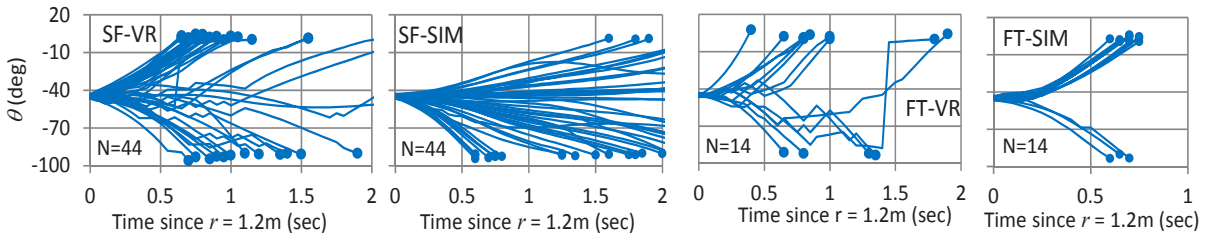

Fig. 15. Relationship between elapsed time and θ. SIM = Simulated, Angles of incidence are between −43° and −47° . Scenario is C. Dots indicate exit points. Vertical axis is common for all graphs.

6. Discussions and Concluding Remarks

The purpose of this study was to investigate whether the anticipated disutility is an essential factor in the models that determine pedestrian movements. The analysis of this study was based on the disutility minimisation principle, i.e., the assumption that the pedestrians select their trajectories so as to minimise their disutility of walking. To perform this purpose, both the theoretical analysis and experimental study with the VR system was conducted.

The results of theoretical analysis imply that incorporating anticipated disutility for walking is necessary to build a model that can reproduce smooth trajectory of pedestrians who avoid other pedestrians. It was shown that the conventional SF model is identical to the instantaneous disutility model, while it is not compatible with the anticipated disutility model. Then, by the numerical test, it was exhibited that a few conventional SF models

create unrealistic trajectories including 'bumping' behaviour when pedestrians try to avoid another pedestrian. These results imply that, if actual pedestrians smoothly avoid other pedestrians in the real world, the instantaneous utility model seems not to be able to correctly reproduce pedestrians' movements in a crowd at the operational level. On the other hand, the models not belonging to the conventional SF model (e.g. models by Johansson et al. [13] and Asano et al. [17]) seem to be able to correctly reproduce smooth avoiding behaviour of pedestrians. As these models explicitly or implicitly incorporate anticipated disutility, it can be concluded that the anticipated utility is an essential factor to reproduce realistic pedestrian movements.

The VR experiment was then carried out to examine the walking behaviour of actual pedestrians. Walking behaviour of the actual pedestrians (VR participant) was compared with the movements of simulated pedestrians (simulated participant) using the restarting procedure. The results showed that, when a pedestrian is approaching to another pedestrian walking perpendicularly, trajectories of simulated participants with the conventional SF model were similar to the 'bumping' movements, whereas simulated participants with the FT model and VR participants (i.e. actual human) with the FT or SF model were not so but smoothly avoid the opponent. These observations imply that the pedestrians in the real world follow the anticipated disutility model.

As the main result of this study, owing to the results shown above, we can state that 'the anticipated disutility is an essential factor in the models that determine pedestrian movements with the disutility minimisation principle'. Using the model that explicitly considers the anticipatory behaviour is a solution to propose a proper model – this approach has been taken by [17] [18] [19]. Alternatively, one can expand the conventional SF model so that it incorporates the anticipatory behaviour like the studies of [11], [13], and [14]. The findings of the present study emphasises the value of these studies incorporating the anticipatory behaviour in the microscopic pedestrian movement models.

There are several tasks to do to investigate the mechanisms of microscopic pedestrian behaviour. The VR technique for the pedestrian behavioural study should be further investigated and improved to ensure that the technique can reproduce the pedestrians' behaviour in the real world more precisely. One issue would be how to ensure the reality of proximity disutility between a participant and simulated pedestrians in the system. The other issue would be how to collect data of participants' movements by sensors. In the current version of the VR system, participants needed to step without moving – this is, of course, not natural. In addition, the speed control of walking is limited in the current version of the system. These limitations may affect the result. Improving the VR systems and/or investigating differences from pedestrians movements in the actual walking space should be accomplished in future studies. The restarting procedure was a powerful tool for the purpose of this study, but is not very suitable to perform a quantitative estimation of model parameters (like a study by Hoogendoorn and Daamen [23] or Robin et al. [24]). We may also need to develop a new technique to do it by the VR technique. The result implying the importance of anticipation requests studies that investigate how actual pedestrians anticipate others' movements in the next few second. There may be many approaches to investigate this issue. Investigating the SF-based models that implicitly consider anticipatory behaviour such as [13] would be worthwhile for this purpose because such models can reproduce anticipatory behaviour with no explicit incorporation of pedestrians' future positions. Interpreting these models by the utility maximisation principle would provide hints to understand how people anticipate others' future movements by seeing current positions and velocities. Assuming that actual pedestrians can gain the ability to anticipation others' movements by learning would be another approach. We may be able to apply the evolution game theory in future studies that try to model the microscopic behaviour of pedestrians and any form of vehicles that can run around two-dimensional space.

Acknowledgements

This study is financially supported by JSPS Grant-in-Aid #22686048.

References

[1] Algadhi, S. A. H. and Mahmassani, H. S. (1990). Modelling crowd behavior and movement: application to Makkah pilgrimage. In M. Koshi (Ed.). Transportation and Traffic Theory (pp.59-78), Elsevier.
[2] Hughes, R. L. (2002). A continuum theory for the flow of pedestrians. Transportation Research Part B, 36, pp.507-535.
[3] Huang, L., Wong, S.C., Zhang, M., Shu, C.W. and Lam, W.H.K. (2009). Revisiting Hughes' dynamic continuum model for pedestrian flow and the development of an efficient solution algorithm. Transportation Research Part B: Methodological, 43(1), pp.127-141.
[4] Lam, W. H. K., Lee, J. Y. S., Chan, K. S. and Goh, P. K. (2003). A generalised function for modeling bi-directional flow effects on indoor walkways in Hong Kong. Transportation Research Part A, 37: pp.789–810.
[5] Helbing, D., Buzna, L., Johansson, A. and Werner, T. (2005). Self-Organized Pedestrian Crowd Dynamics: Experiments, Simulations, and Design Solutions. Transportation Science, 39(1), pp.1-24
[6] Hoogendoorn S.P. and Bovy, P.H.L. (2004). Pedestrian route-choice and activity scheduling theory and models. Transportation Research Part B, 38, pp.169-190.
[7] Wardrop, J. G. (1952). Some theoretical aspects of road traffic research. Proceedings of the Institute of Civil Engineers, Part II, pp. 325–378.
[8] Hoogendoorn, S. and Bovy, P.H.L. (2003). Simulation of pedestrian flows by optimal control and differential games. Optimal Control Applications and Methods, 24(3), pp.153-172.
[9] Helbing, D. and Molnár, P. (1995). Social force model for pedestrian dynamics. Physical Review E, 51(5), pp.4282-4286.
[10] Helbing, D., Farkas, I. and Vicsek, T. (2000). Simulating dynamical features of escape panic. Nature, 407, pp. 487-490.
[11] Lakoba, T.I. Kaup, D.J., and Finkelstein, N.M. (2005). Modifications of the Helbing-Molnar-Farkas-Vicsek Social Force Model for Pedestrian Evolution. Simulation, 81(5), pp.339-352.
[12] Seyfried, A., Steffen, B. & Lippert, T. (2006). Basics of modelling the pedestrian flow. Physica A: Statistical Mechanics and its Applications, 368(1), pp.232-238.
[13] Johansson, A., Helbing, D., and Shukla, P. K. (2007). Specification of the Social Force Pedestrian Model by Evolutionary Adjustment to Video Tracking Data. Advances in Complex Systems, 10(2), pp. 271-288.
[14] Parisi, D.R., Gilman, M. and Moldovan, H. (2009). A modification of the Social Force Model can reproduce experimental data of pedestrian flows in normal conditions. Physica A: Statistical Mechanics and its Applications, 388(17), pp.3600-3608.
[15] Löhner, R. (2010). On the modeling of pedestrian motion. Applied Mathematical Modelling. 34(2), pp.366-382.
[16] Suma, Y., Yanagisawa, D. and Nishinari, K. (2012). Anticipation effect in pedestrian dynamics: Modeling and experiments. Physica A: Statistical Mechanics and its Applications, 391(1-2), pp.248-263.
[17] Asano, M., Iryo, T. and Kuwahara, M. (2009). A pedestrian model considering anticipatory behaviour for capacity evaluation. In W. H. K. Lam, S. C. Wong and H. K. Lo (Eds.), Transportation and Traffic Theory 2009: Golden Jubilee (pp. 559-581), New York: Springer.
[18] Asano M., Iryo T. and Kuwahara, M. (2010). Microscopic pedestrian simulation model combined with a tactical model for route choice behaviour. Transportation Research Part C, 18, pp. 842-855.
[19] Moussaïd, M., D. Helbing and G. Theraulaza (2011). How simple rules determine pedestrian behavior and crowd disasters. Proceedings of the National Academy of Science of the United States of America, 108(17), pp. 6884–6888.
[20] Louloudi, A. and Klügl, F. (2011). Visualizing agent-based simulation dynamics in a CAVE - issues and architectures. In Proceedings of the Federated Conference on Computer Science and Information Systems. pp. 651-658.
[21] Kretz, T., Hengst, S., Arias, A. P., Friedberger, S., Hanebeck, U. D. (2012). Using extended range telepresence to collect data of pedestrian dynamics. 91st Transportation Research Board Annual Meeting, Washington D.C., DVD-ROM.
[22] Lam, W. H. K., Morrall, J. F. and Ho, H. (1995). Pedestrian flow characteristics in Hong Kong. Transportation Research Record, 1487, pp. 56-62.
[23] Hoogendoorn, S. P. and Daamen, W. (2009). A novel calibration approach of microscopic pedestrian models. in: H. Timmerman (Ed.) Pedestrian Behavior: Models, Data Collection and Applications, Emerald Group Publishing Limited: pp.195-214.
[24] Robin, T., Antonini, G. Bierlaire, M. and Cruz, J. (2009). Specification, estimation and validation of a pedestrian walking behavior model. Transportation Research Part B 43(1): pp. 36-56.
[25] Gebhardt, N. et al. Irrlicht Engine - A free open source 3D engine. http://irrlicht.sourceforge.net/, retrieved on 2012/08/12.